On the determination of the He abundance distribution in globular clusters from the width of the main sequence

Santi Cassisi,[1,2]★ Maurizio Salaris,[3] Adriano Pietrinferni[1] and David Hyder[3]

[1]*INAF – Osservatorio Astronomico di Teramo, Via M. Maggini, I-64100 Teramo, Italy*
[2]*Instituto de Astrofísica de Canarias, Calle Via Lactea s/n, E-38205 La Laguna, Tenerife, Spain*
[3]*Astrophysics Research Institute, Liverpool John Moores University, IC2, Liverpool Science Park, 146 Brownlow Hill, Liverpool L3 5RF, UK*

ABSTRACT

One crucial piece of information to study the origin of multiple stellar populations in globular clusters is the range of initial helium abundances ΔY amongst the sub-populations hosted by each cluster. These estimates are commonly obtained by measuring the width in colour of the unevolved main sequence in an optical colour–magnitude diagram (CMD). The measured colour spread is then compared with predictions from theoretical stellar isochrones with varying initial He abundances to determine ΔY. The availability of UV/optical magnitudes, thanks to the *Hubble Space Telescope* UV Legacy Survey of Galactic GCs project, will allow the homogeneous determination of ΔY for a large Galactic globular cluster sample. From a theoretical point of view, accurate UV CMDs can efficiently disentangle the various sub-populations, and main sequence colour differences in the ACS $F606W - (F606W - F814W)$ diagram allow an estimate of ΔY. We demonstrate that from a theoretical perspective, the $(F606W - F814W)$ colour is an extremely reliable He-abundance indicator. The derivative $dY/d(F606W - F814W)$, computed at a fixed luminosity along the unevolved main sequence, is largely insensitive to the physical assumptions made in stellar model computations, being more sensitive to the choice of the bolometric correction scale, and is only slightly dependent on the adopted set of stellar models. From a theoretical point of view, the $(F606W - F814W)$ colour width of the cluster main sequence is therefore a robust diagnostic of the ΔY range.

Key words: stars: abundances – stars: low-mass – globular clusters: general.

1 INTRODUCTION

During the last fifteen years, our understanding of Galactic globular clusters (GGCs) has been revolutionized by a plethora of observational evidence, based on both photometric and spectroscopic surveys. The long-standing paradigm that considered these stellar systems as prototypes of simple (single age, single initial chemical composition) stellar populations is no longer valid. Indeed GGCs (and old extragalactic globular clusters) host a first population with initial chemical abundance ratios similar to the one of field halo stars, and additional distinct sub-populations, each one characterized by its own specific variations of the abundances of He, C, N, O, Na, and sometimes Mg and Al (see, e.g. Gratton, Sneden & Carretta 2004), compared to the field halo abundance ratios.

These abundance patterns give origin, within individual clusters, to well-defined (anti)correlations between pairs of light elements, the most characteristic one being the Na–O anticorrelation, nowadays considered the most prominent signature for the presence of multiple populations in a given GGC.

According to the currently most debated scenarios, the observed light element variations are believed to be produced by high-temperature proton captures either at the bottom of the convective envelope of massive asymptotic giant branch (AGB) stars (see, e.g. D'Ercole et al. 2008), or in the cores of main sequence (MS) fast-rotating massive stars (FRMSs – see, e.g. Decressin et al. 2007), or supermassive stars (SMSs – see Denissenkov & Hartwick 2014; Denissenkov et al. 2015), belonging to the cluster first population. The CNO-processed matter is then transported to the surface either by convection (in AGB stars and the fully convective SMSs) or rotational mixing (in FRMSs), and injected in the intracluster medium by stellar winds. According to these scenarios, the other cluster sub-populations are generally envisaged to have formed out of this gas, with a time delay (of the order of at most 10^8 yr) that depends on the type of polluter. Age delays so small, if present, are basically impossible to detect from the clusters' colour–magnitude diagrams (CMDs).

According to the AGB scenario, the observed variation of He amongst stars in the same cluster is due to the CNO-processed ejecta that are also enriched in He due mainly to the effect of the second dredge up during the early AGB phase. According to the FRMS and SMS scenario, the increase of He comes from the

★ E-mail: cassisi@oa-teramo.inaf.it

same core H-burning that produces the light element variations. Most importantly, AGB, FRMS and SMS scenarios predict different relationships between light element and He abundance variations. Accurate estimates of the He abundance range within individual GGCs is therefore crucial to constrain the origin of the multiple population phenomenon (see, e.g. Bastian, Cabrera-Ziri & Salaris 2015; Tenorio-Tagle et al. 2016).

He abundance variations (hereafter ΔY, whereas usual Y denotes the helium mass fraction) can, in principle, be determined by direct spectroscopic measurements in bright, low-gravity red giant branch (RGB) stars and hot horizontal branch (HB) stars. In case of the RGB stars, ΔY estimates (obtained so far for NGC 2808 and ω Centauri) are based on measurements of the near-infrared He I 10 830 Å chromospheric line (see Dupree, Strader & Smith 2011; Pasquini et al. 2011; Dupree & Avrett 2013). Uncertainties related to the necessary non-local thermodynamics equilibrium corrections and chromospheric modelling somewhat limit the current accuracy of this diagnostic.

Spectroscopic measurements of the He abundance in HB stars (see, e.g. Villanova et al. 2012; Marino et al. 2014; Mucciarelli et al. 2014, and references therein) are based on several photospheric He lines that are excited in HB stars hotter than ∼8500 K, but only objects between this lower $T_{\rm eff}$ limit and an upper limit of about 11 500–12 000 K are appropriate targets. Above this $T_{\rm eff}$ threshold, the gravitational settling of He sets in (see, e.g. Moni Bidin et al. 2007; Moehler et al. 2011, 2014) and the measured abundances would be much lower than the initial values[1]. These requirements about the $T_{\rm eff}$ of the targets hamper the use of this method to estimate reliably ΔY ranges for the following reasons. First of all, not all GGCs host HB stars that reach $T_{\rm eff} = 8500$ K (a typical example is the metal-rich cluster 47 Tucanae). Secondly, in GGCs, with an extended HB, the various sub-populations show some kind of colour segregation along the branch. The first population with primordial He abundance is preferentially located at the red side of the HB, whilst sub-populations with increasing degree of variations of the light element abundances (hence presumably He) are distributed towards the hotter end of the HB (see, e.g. Marino et al. 2011; Gratton et al. 2013). This implies that the $T_{\rm eff}$ window suitable to determine Y in HB stars cannot sample the full ΔY range in the cluster.

The presence of He-enhanced stellar populations affects also the CMD of GGCs, and indeed, the existence of a range of initial He abundances within individual GGCs was first inferred from the optical CMD of MS stars in ω Centauri (Bedin et al. 2004; Norris 2004; King et al. 2012) and NGC 2808 (Piotto et al. 2007). The details of the techniques applied to determine ΔY ranges from CMDs vary from author to author (compare, for example, the methods applied by King et al. 2012; Milone et al. 2012, 2015), but they are all based on the following properties of stellar models/isochrones.

It is well established that an increase of the initial He abundance in MS stars of a given mass changes their $T_{\rm eff}$ as a consequence of the associated decrease of the envelope radiative opacities, so that they become hotter with increasing Y. At the same time, an increase of Y increases the molecular weight of the stellar gas and makes MS

stars of a given mass also brighter (see, e.g. Kippenhahn, Weigert & Weiss 2012; Cassisi & Salaris 2013). The net effect is that, at a given brightness, the unevolved MS of theoretical isochrones with increasing He abundances (and fixed metal content) become progressively bluer.

In addition, Salaris et al. (2006), Sbordone et al. (2011) and Cassisi et al. (2013) have shown that optical CMDs of GGCs are expected to display multiple MS sequences only if the different populations are characterized by variations of Y. The reason is that for a given Y, standard α-enhanced isochrones (from the MS to the tip of the RGB) that match the metal composition of the cluster first population are identical to isochrones that include the full range of observed light element variations. Moreover, the same light element abundance variations (and variations of Y) do not affect the bolometric corrections (BCs) to optical photometric filters (see Girardi et al. 2007; Sbordone et al. 2011).

To summarize, it is possible to safely determine the range ΔY in individual GGCs by comparing theoretical MS isochrones with standard α-enhanced metal distributions and varying initial Y to cluster optical CMDs. Once photometric errors (and eventually differential reddening and unresolved binaries) are taken into account, the observed width of the unevolved MS provides an estimate of ΔY amongst the cluster multiple populations.

This method can be applied to all clusters with available accurate optical photometry provided that the various sub-populations have been identified (as discussed below). The colour separation of their respective MSs is an especially reliable ΔY diagnostic, based on a simple and well-modelled evolutionary phase. Other methods based on cluster photometry, such as comparisons of the predicted and observed brightness of the luminosity function RGB bump (see, e.g. Milone et al. 2015) and the analysis of the HB morphology and brightness with synthetic HB models (see, e.g. Dalessandro et al. 2013; Gratton et al. 2013) rely on models of more advanced evolutionary phases, and potentially subject to larger systematic errors.

In this paper, we study the robustness of the theoretical calibration of MS colour versus initial Y in optical filters, in view of its relevance for the quest of the origin of the multiple populations in globular clusters, and the availability of a large sample of high-precision UV-optical CMDs from the *Hubble Space Telescope* UV Legacy Survey of Galactic GCs. This survey has observed 54 GGCs through the filters *F275W*, *F336W*, *F438W* of the Wide Field Camera 3 (WFC3) on-board *Hubble Space Telescope* (*HST*; Piotto et al. 2015) and its results must be used in conjunction with the existing *F606W* and *F814W* extensive and homogeneous photometry from the *HST*/ACS GGC Treasury project (see Sarajedini et al. 2007) to identify the various sub-populations hosted by individual clusters (see, e.g. Milone et al. 2015; Nardiello et al. 2015, and references therein) and determine ΔY homogeneously, for a large GGC sample. The use of UV filters maximizes the colour separation between the various populations in individual clusters (because the CNONa variations affect the BCs in UV filters) and after the different MS components are clearly identified in the UV, their (smaller) colour separation in optical filters provides ΔY on a cluster-by-cluster basis.

Bastian et al. (2015) have shown how none of the proposed AGB-, FRMS- or SMS-based scenarios are able to match simultaneously ΔY and the observed range of the O–Na anticorrelation in a small sample of GGCs where ΔY estimates are available, questioning the reliability of our current ideas about the formation of cluster multiple populations. An homogeneous determination of ΔY for a large sample of GGCs is strongly required to confirm or disprove this result and this will be done within the *Hubble Space*

---

[1] In case of both RGB and HB spectroscopy, the measured He abundances are equal to the initial values, plus the small increase due to the first dredge up that can be easily predicted by stellar models. In case of efficient atomic diffusion during the MS, the RGB surface He abundances after the first dredge up are slightly lower than the initial ones (Proffitt & Vandenberg 1991).

Telescope UV Legacy Survey of Galactic GCs project. Our analysis aims at assessing the sources of theoretical systematic errors involved in the determination of ΔY from MS photometry in optical *HST*-ACS CMDs, using theoretical stellar isochrones. We focus the analysis that follows on the ACS $F606W - (F606W - F814W)$ CMD (that roughly corresponds to the Johnson–Cousins *VI* CMD), because these are the only filters available within the survey that are completely unaffected by the presence of CNONa abundance variations. The UV filters but also the WFC3 $F438W$ filter (or the $F435W$ ACS counterpart) are sensitive –albeit to different degrees– to these abundance variations (see, e.g. Piotto et al. 2015). In particular, using the theoretical spectra by Sbordone et al. (2011) for $[Fe/H] = -1.6$ for an unevolved MS star along a 12 Gyr isochrone (with $T_{eff} = 4621$ and surface gravity $\log(g) = 4.77$, both for a first population standard α-enhanced mixture and composition with CNONa anticorrelations at constant CNO sum), we found a difference of about 0.05 mag between the corresponding BCs for the WFC3 $F438W$ filter (and the ACS $F435W$ counterpart), whereas the same differences are $\sim$0.001 mag for both the $F606W$ and $F814W$ ACS filters. This confirms that the observed intrinsic colour range of the MS in the ACS $F606W - (F606W - F814W)$ CMD is due to Y differences, irrespective of the exact values of the C, N, O, Na abundances.

The plan of the paper is as follows: Section 2 presents the reference evolutionary framework and the additional isochrone sets computed to study the effect of various physics inputs on the derived ΔY; Section 3 compares the various isochrones sets to establish the robustness of the MS dY/d(colour) derivatives. A critical summary of the results will close the paper.

2 THE THEORETICAL MODELS

The stellar models and isochrones employed in our analysis have been computed with the BaSTI stellar evolution code and our reference calculations employ the input physics and BCs fully described in Pietrinferni et al. (2004, 2006). We have explored a large metallicity range, from $[Fe/H] = -2.1$ to $[Fe/H] = -0.7$ ($[\alpha/Fe] = 0.4$), that covers most of the metallicity range spanned by the GGC population. In the following, we detail the case with $[Fe/H] = -1.3$, representative of the results that we obtain at all metallicities.

More in detail, we calculated models and isochrones (neglecting the effect of atomic diffusion) with metal mass fraction $Z = 0.002$, $Y = 0.248$ and $[\alpha/Fe] = 0.4$, corresponding to $[Fe/H] = -1.3$, that represent the first population in a cluster with this $[Fe/H]$. In addition we calculated models and isochrones for the same Z and α-enhancement, but with $Y = 0.30$, 0.35 and 0.40, respectively, corresponding to sub-populations with increasing initial He abundance[2].

It is important to clarify the choice of varying Y in the models while keeping Z fixed, instead of keeping $[Fe/H]$ fixed. The observed abundance patterns do not change the total metallicity Z. This is essentially because the sum of the CNO abundances plus the abundances of all elements not affected by the anticorrelations (chiefly amongst them Ne, Fe and Si) makes about 90 per cent or more of the metal content by mass, and is unchanged amongst the cluster sub-populations, with the exception of a few cases like NGC 1851 (Yong, Grundahl & Norris 2015), NGC 6656 (Marino et al. 2012a) and ω Centauri (Marino et al. 2012b). At the same time,
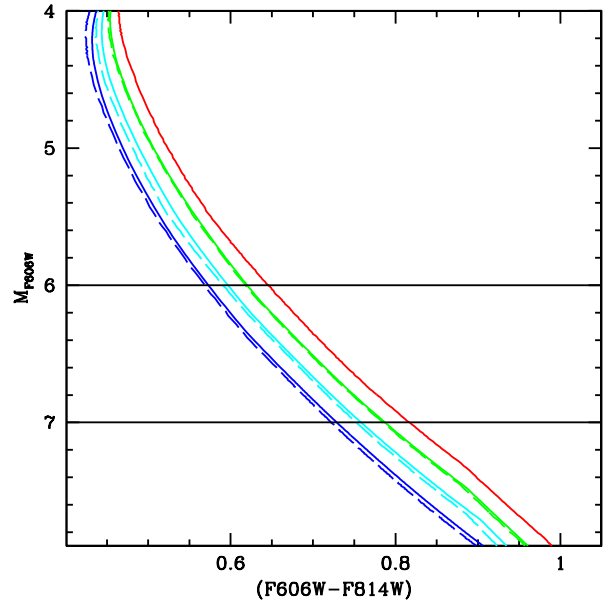

Figure 1. A set of our reference MS isochrones (calculated at fixed Z) for an age of 12 Gyr and (moving towards bluer colours) $Y = 0.248$, 0.30, 0.35, 0.40, respectively (solid lines), compared to MS isochrones calculated with the same age and Y values, but keeping $[Fe/H]$ constant (dashed lines – see the text for details).

as shown by Bragaglia et al. (2010), when the range of Y amongst the cluster sub-populations is sufficiently large, it is possible to detect corresponding small variations of $[Fe/H]$ consistent with the expected change due to the variation of the hydrogen abundance (note that $\Delta Y = 0.1$ at fixed Fe corresponds to $\Delta[Fe/H] \sim 0.06$).

As already stated, we focus the analysis that follows on the $F606W - (F606W - F814W)$ CMD, based on *HST*-ACS filters. As mentioned in the introduction, light element variations do not affect BCs to these filters, and moreover, the $(F606W - F814W)$–T_{eff} relation is very weakly dependent on metallicity, as we have also verified with our adopted reference BCs based on ATLAS9 model atmospheres and spectra (see Pietrinferni et al. 2004). This means that the predicted MS colour shifts in this CMD are more closely related to the T_{eff} shifts caused by Y variations, and also that scaled solar BCs, with either the same total metallicity or the same $[Fe/H]$ of the α-enhanced composition, can be safely used (if the appropriate α-enhanced BCs are unavailable) as demonstrated in fig. 1 of Cassisi et al. (2004). The BCs applied to our isochrones have been calculated for the $[Fe/H]$ of the normal Y composition (the lowest Y value) and kept unchanged for the He-enhanced isochrones, because they are unaffected by a change of Y when the total metal content is kept constant (and they are unaffected by the CNONa anticorrelations – see Section 1).

Fig. 1 displays the MS of a set of our reference isochrones, for an age of 12 Gyr and varying Y. The horizontal lines mark $M_{F606W} = 6$ and 7, respectively, the two magnitude levels along the unevolved MS – more than $\sim$2 mag below the turn-off level – where we will calculate the derivative $dY/d(F606W - F814W)$ and discuss its uncertainties[3]. The same figure shows, for the sake of

---

[2] All these stellar models and isochrones are available at the BaSTI url site: http://www.oa-teramo.inaf.it/BASTI

[3] We have obtained quantitatively the same fractional uncertainties on $dY/d(F606W - F814W)$ when we considered as reference magnitudes $M_{F814W} = 5.6$ and 6.6, corresponding to $\sim$2 and $\sim$3 mag below the MS turn-off in the $F814W$ filter.

comparison, isochrones calculated for the same age and initial Y values, but keeping [Fe/H] $= -1.3$ for all Y – hence Z decreases with increasing Y, by at most $\sim$15 per cent. For ΔY up to $\sim$0.05, there is essentially no difference between the case of keeping Z or [Fe/H] fixed. Differences appear when $\Delta Y > 0.05$ and increase with increasing Y, due to the fact that Z must be decreased by increasingly larger values in order to keep [Fe/H] unchanged. As a result, employing theoretical MSs at varying Y and [Fe/H] fixed would lead to systematically smaller ΔY values, when $\Delta Y > 0.05$.

For our reference isochrones, at $M_{F606W} = 7$, the evolving mass along the $Y = 0.248$ MS is equal to $0.57\,M_\odot$, decreasing to $0.46\,M_\odot$ along the $Y = 0.40$ MS. At $M_{F606W} = 6$, the evolving masses are equal to 0.65 and $0.52\,M_\odot$, respectively. The MSs with higher initial Y are bluer at a given M_{F606W} and the colour differences between pairs of MSs with different initial Y tend to slowly decrease moving to brighter magnitudes.

From these isochrones, we obtain $\mathrm{d}Y/\mathrm{d}(F606W - F814W) = 1.8$ at $M_{F606W} = 7$ and $\mathrm{d}Y/\mathrm{d}(F606W - F814W) = 2.1$ at $M_{F606W} = 6$, irrespective of the value of Y, within the range $Y = 0.248$–0.40. These derived values of $\mathrm{d}Y/\mathrm{d}(F606W - F814W)$ are, as expected, insensitive to the adopted isochrone age t. We have actually verified that variations of t by ± 1–2 Gyr around $t = 12$ Gyr do not affect $\mathrm{d}Y/\mathrm{d}(F606W - F814W)$ at both $M_{F606W} = 6$ and 7.

We have then calculated additional isochrones for the same Z and the same Y range, but varying one at a time the following inputs that affect the CMD location of evolutionary tracks and isochrones.

(i) The BCs adopted to compare theoretical isochrones with observed CMDs;

(ii) the efficiency of convection in the outer, superadiabatic layers, e.g. the value of the mixing length parameter α_{MLT} employed in the model computations;

(iii) the outer boundary conditions employed in the stellar model calculations;

(iv) inclusion of fully efficient atomic diffusion everywhere in the models or just below the convective envelope.

With these model computations, we have calculated appropriate sets of isochrones, to assess the robustness of the $\mathrm{d}Y/\mathrm{d}(F606W - F814)$ predictions that will be discussed in the next section.

Finally, to explore the effect of using independent evolutionary calculations – that employ also some different choices of physics inputs – we considered the Dell'Omodarme et al. (2012) and VandenBerg et al. (2014) models that provide isochrones at fixed Z and varying Y values for several ages.

3 ANALYSIS

For all additional sets of isochrones listed in the previous section, we have determined $\mathrm{d}Y/\mathrm{d}(F606W - F814W)$ at both $M_{F606W} = 6$ and 7, and compared these values with the results from the reference set. The results of these comparisons are discussed in the following sections, considering separately each one of the new sets.

3.1 Bolometric corrections

To study the effect of varying the BCs, we employed the theoretical values calculated with the PHOENIX and MARCS model atmosphere codes (see Brott & Hauschildt 2005; Casagrande & VandenBerg 2014), respectively, and the empirical BCs by Worthey & Lee (2011). Worthey & Lee (2011) provide BCs to the Johnson–Cousins VI filters that we have translated to the corresponding ACS filters using the empirical relationships by Sirianni et al. (2005).
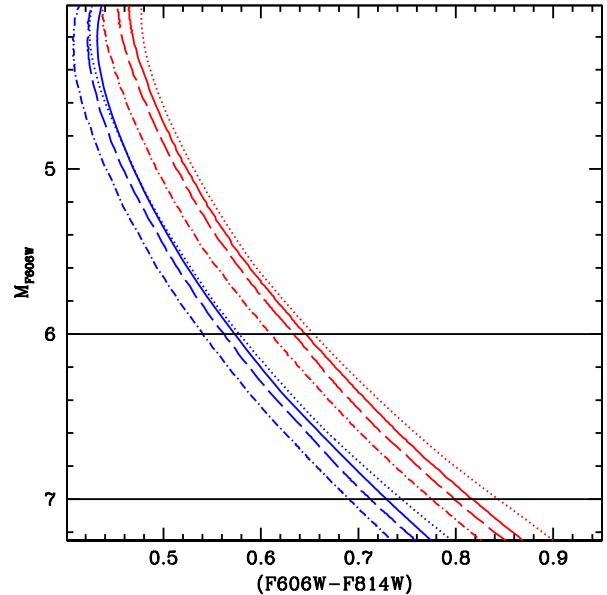

Figure 2. Comparison of 12 Gyr MS isochrones for $Y = 0.248$ and 0.40. We display our reference isochrones (with ATLAS9 bolometric corrections, solid lines) and the same isochrones but applying alternative empirical (dotted lines) and theoretical (PHOENIX as dashed lines, MARCS as dash–dotted lines) bolometric corrections, respectively (see the text for details).

Both PHOENIX- and MARCS-based BCs are calculated for an α-enhanced [α/Fe] $= 0.4$ metal mixture; however, the reference solar heavy element distribution for the available MARCS models is from Grevesse, Asplund & Sauval (2007), instead of Grevesse & Noels (1993) as for PHOENIX and our reference ATLAS9 BCs. This difference may possibly add a degree of inconsistency to the results of this comparison.

Fig. 2 compares these new sets of isochrones with the reference ones, for $Y = 0.248$ and 0.40 (the extreme values of the range spanned by our calculations), $t = 12$ Gyr. The PHOENIX and MARCS BCs produce MSs bluer by about 0.015 and 0.04 mag, respectively, at all M_{F606W}, compared to the reference set. The shift is the same for both values of Y, and as a consequence, we find that $\mathrm{d}Y/\mathrm{d}(F606W - F814W)$ stays unchanged compared to the reference values at $M_{F606W} = 6$ and 7.

The results employing the empirical BCs by Worthey & Lee (2011) are different. In this case, it is evident from Fig. 2 that there is a shift in the MS colours (generally redder than the reference isochrones) but also a clear change of shape. We obtain $\mathrm{d}Y/\mathrm{d}(F606W - F814W) = 2.0$ and 1.5 – irrespective if Y – at $M_{F606W} = 6$ and 7, respectively. The difference with respect to the reference derivatives are larger at the fainter magnitude level.

3.2 The value of α_{MLT} and the outer boundary conditions

The mixing length theory (MLT – Böhm-Vitense 1958) is almost universally used to compute the temperature gradient in superadiabatic layers of stellar (interior and atmosphere) models. This formalism contains in its standard form four free parameters. Three parameters are fixed a priori (and define what we denote as the MLT flavour), whereas one (the so-called mixing length, α_{MLT}) is calibrated by reproducing observational constraints (see, e.g. Salaris & Cassisi 2008, and references therein). In our reference calculations, we have employed the Cox & Giuli (1968) implementation of the MLT (corresponding to the ML1 flavour described in Salaris &

Cassisi 2008) with α_{MLT} fixed by the standard solar model calibration (see Pietrinferni et al. 2004, for details).

In these additional sets of isochrones, we have considered a variation of α_{MLT} by ± 0.1 around the solar value. This is consistent with the variation of α_{MLT} along the isochrone MS predicted by the 3D radiation hydrodynamics simulations by Magic, Weiss & Asplund (2015). We find that at fixed Y, the three sets of MSs are virtually coincident for $M_{F606W} \sim 6$ and fainter magnitudes. The reason is that models in this magnitude range have deep convective envelopes almost completely adiabatic and the variation of α_{MLT} has a very minor effect on their temperature stratification. As a result, $dY/d(F606W - F814W)$ values are unchanged.

Given that the envelopes of stellar models in this magnitude range are almost completely adiabatic, we expect a negligible difference when employing alternatively the Canuto & Mazzitelli (1991) theory of superadiabatic convection, instead of the MLT. This is confirmed by fig. A2 in Mazzitelli, D'Antona & Caloi (1995) that compares in the L–T_{eff} diagram GGC isochrones calculated with a solar-calibrated mixing length and with the Canuto & Mazzitelli (1991) formalism. In the relevant L range (between $\log(L/L_{\odot}) \sim -0.5$ and ~ -0.9), the two sets of MS isochrones at a given initial chemical composition are virtually indistinguishable.

Regarding the model outer boundary conditions, we recall that to integrate the stellar structure equations, it is necessary to fix the value of the pressure and temperature at the surface of the star, usually close to the photosphere (see, e.g. VandenBerg et al. 2008, and references therein). In our reference calculations, we have determined this boundary condition by integrating the atmospheric layers using the solar Krishna Swamy (1966) $T(\tau)$ relation, supplemented by the hydrostatic equilibrium condition and the equation of state. The choice of the outer boundary conditions is important in this context, because it affects the T_{eff} of stellar models with convective envelopes (see, e.g. Cassisi & Salaris 2013; Salaris & Cassisi 2015, for more details)

In this additional set of MS isochrones, we have employed the Eddington grey $T(\tau)$ instead. We have first recalibrated the solar value of the mixing length α_{MLT} with this $T(\tau)$ relation and then calculated models and isochrones with the new solar-calibrated mixing length (about 0.1 smaller than the value calibrated with the reference $T(\tau)$ relation).

Fig. 3 compares these new calculations with the reference one for the same selected t and Y values employed in the previous comparisons. The MSs calculated with the Eddington $T(\tau)$ are systematically bluer (by about 0.02 mag), but the shift is independent of Y and the MS shape is preserved. As a consequence, $dY/d(F606W - F814W)$ values are unchanged compared to the reference case.

3.3 The efficiency of atomic diffusion

Asteroseismic data require the inclusion of atomic diffusion in standard solar model calculations, to match the inferred solar sound–speed profile, depth of the convective envelope and surface He abundance (see, e.g. Bahcall, Pinsonneault & Wasserburg 1995; Villante et al. 2014, and references therein). The situation for GGC stars is, however, very different. Spectroscopic determinations of metal abundances from the MS turn-off to the RGB of a number of GGCs have shown that the efficiency of atomic diffusion from the convective envelope of old metal poor stars is severely reduced (see, e.g. Gratton et al. 2001; Lind et al. 2008; Mucciarelli et al. 2011; Gruyters, Nordlander & Korn 2014, and references therein) by some as yet unspecified competing physical process. Nothing is
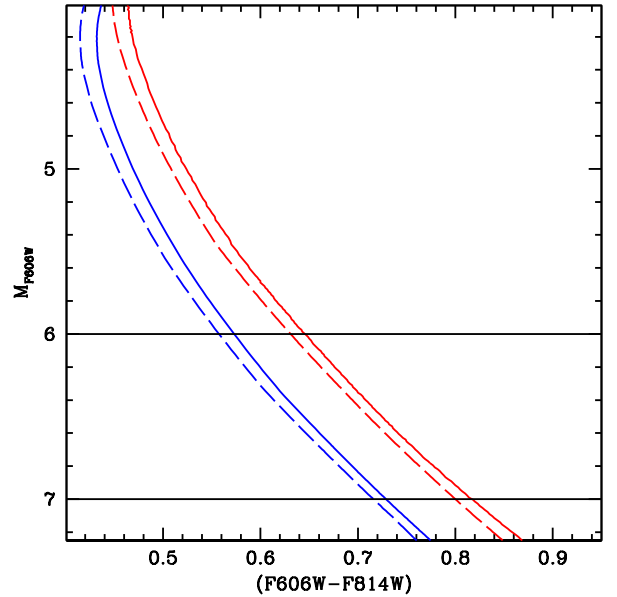

Figure 3. As Fig. 2 but displaying our reference isochrones (solid lines) and isochrones calculated using the Eddington grey $T(\tau)$ for the outer boundary conditions (dashed lines – see the text for details).

known about the efficiency of diffusion in the radiative interiors of these objects.

To study the potential impact on $dY/d(F606W - F814W)$, we have therefore calculated two sets of isochrones. The first one includes fully efficient diffusion throughout the stellar models (we employed the diffusion coefficient by Thoul, Bahcall & Loeb 1994, implemented in the BaSTI code) and one including efficient atomic diffusion only below the boundary of the convective envelope.

The set with fully efficient diffusion is an extreme and, for what we know, unrealistic case for GGC stars, but necessary to understand the comparisons with $dY/d(F606W - F814W)$ values obtained with other theoretical isochrones that include atomic diffusion (see the next section). Regarding the models with artificially inhibited diffusion from the envelope, starting at a distance of $0.5H_P$ (where H_p is the pressure scaleheight at the Schwarzschild boundary of the convective envelope) below the surface convection boundary, we smoothly reduced the diffusion velocities of the various elements (with a quadratic function of radius) so that they reached zero at the bottom of the fully mixed envelope. This second set is a numerical experiment to simulate the inhibition of diffusion from the convective boundary, keeping the element transport efficient in the interiors.

In general, the effect of atomic diffusion on stellar evolution tracks of a given mass (for masses typical of GGCs) and initial chemical composition is to shorten the MS lifetimes by ~1 Gyr due to the diffusion of helium to the centre, that is equivalent to a faster aging of the star. Also, due to the diffusion of He and metals from the convective envelopes, the surface H abundance increases, causing a higher opacity and a shift of the tracks towards redder colours. In addition, the inward settling of helium raises the core molecular weight and the molecular weight gradient between surface and centre of the star, which also contributes to increase the stellar radius (see, e.g. Cassisi et al. 1998; Salaris, Groenewegen & Weiss 2000).

Fig. 4 shows the results of these calculations, compared to the reference case. The displayed isochrones with diffusion are ~1 Gyr younger than the reference one, so that they have approximately
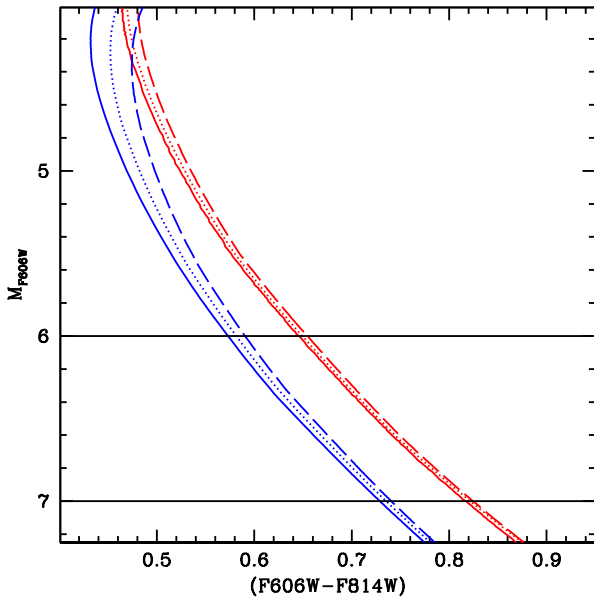
Figure 4. As Fig. 2 but displaying our reference isochrones (solid line), 11 Gyr old isochrones including fully efficient atomic diffusion (dashed lines) and diffusion efficient only below the convective envelope (dotted lines – see the text for details).

Figure 5. Comparison of Dell'Omodarme et al. (2012) and VandenBerg et al. (2014) 12 Gyr, $Z = 0.002$, $Y = 0.25$ isochrones (dotted and dashed lines, respectively) with our reference 12 Gyr, $Z = 0.002$, $Y = 0.248$ isochrone (solid line), in both the L–T_{eff} (upper panel) and $F606W - (F606W - F814W)$ (lower panel) diagrams.

the same MS turn-off magnitude. As for the case of individual tracks, fully efficient atomic diffusion shifts the isochrone MS to redder colours, by an amount that increases moving towards the MS turn-off. Lower MS objects are less affected because of their very extended, fully mixed, convective envelopes that minimize the reduction of surface metals and He. The effect is larger when Y increases, because of generally shallower convective envelopes.

We find that $dY/d(F606W - F814W)$ at $M_{F606W} = 6$ increases compared to the reference value, but only for $Y > 0.30$ whilst it is basically unchanged at $M_{F606W} = 7$, where the effect of diffusion is negligible. When $Y > 0.30$, the value of $dY/d(F606W - F814W)$ in case of fully efficient diffusion depends on the actual value of Y. We find that for Y between 0.30 and 0.35, $dY/d(F606W - F814W) = 2.5$, increasing to 2.6 when Y is between 0.35 and 0.40.

It is instructive to notice that the MS with diffusion from the convective layers inhibited is also shifted to the red compared to reference isochrones, although by a smaller amount compared to the case of fully efficient diffusion. Most importantly, the shifts are Y- and magnitude-independent, and the effect on $dY/d(F606W - F814W)$ is negligible.

3.4 Independent stellar model calculations

We have also considered two publicly available independent sets of stellar evolution models and isochrones that include variations of Y at constant Z, to explore the effect of varying additional input physics. We considered the Dell'Omodarme et al. (2012) and VandenBerg et al. (2014) model data bases.

The Dell'Omodarme et al. (2012) data base provides isochrones in the theoretical L–T_{eff} diagram at fixed Z and varying Y values for several ages. We focused on their 12 Gyr, $Z = 0.002$ isochrones with $Y = 0.25$, 0.33 and 0.38, respectively. They have been calculated for a scaled solar chemical composition and employ the solar mixture by Asplund et al. (2009), different from our reference solar mixture (Grevesse & Noels 1993). These calculations rely also on some physics inputs different from those adopted in our own cal-
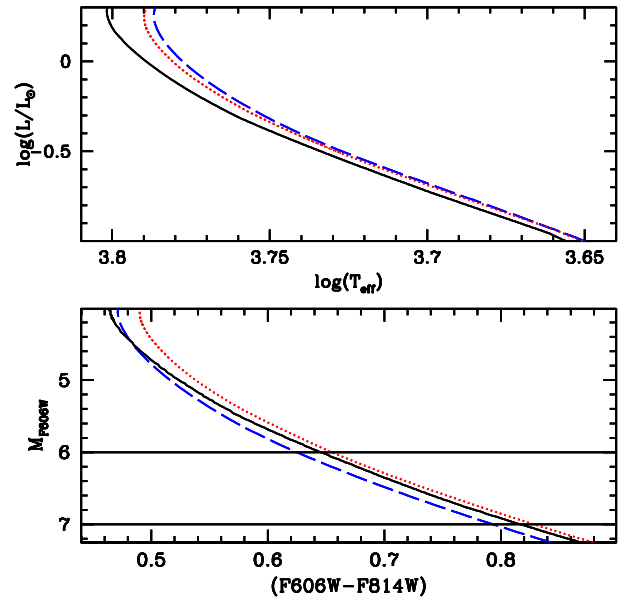
culations. In more detail, Dell'Omodarme et al. (2012) adopted the OPAL equation of state (Rogers, Swenson & Iglesias 1996), whilst our reference calculations employ the freeEOS one (see Cassisi, Salaris & Irwin 2003; Pietrinferni et al. 2004); the outer boundary conditions for MS stars at these metallicity and ages are taken from the PHOENIX model atmospheres (Brott & Hauschildt 2005) instead of a $T(\tau)$ integration. Also, the reaction rate for the $^{14}N(p, \gamma)^{15}O$ reaction is taken from Imbriani et al. (2005), whilst our reference calculations employ the Angulo et al. (1999) rate. Finally, these isochrones include also fully efficient atomic diffusion using Thoul et al. (1994) diffusion coefficients.

We applied to these isochrones our scaled solar ATLAS9 BCs calculated for the Grevesse & Noels (1993) solar mixture. We have verified beforehand, with calculations performed using the ATLAS9 suite of codes (Sbordone et al. 2004), that for MS stars in the T_{eff} and L range relevant to this analysis, the BCs for the $F606W$ and $F814W$ filters are the same when employing the Asplund et al. (2009) or the Grevesse & Noels (1993) solar-heavy element distributions. This means that our reference ATLAS9 BCs are also appropriate for the chemical composition adopted by Dell'Omodarme et al. (2012).

Fig. 5 compares the $Y = 0.25$ isochrone (the only one with initial Y very close to our adopted reference values) to our reference one with $Y = 0.248$. At fixed L, the Dell'Omodarme et al. (2012) isochrone is slightly cooler along the unevolved MS, by about ∼70 K. Differences increase when moving towards the turn-off, because of the inclusion of fully efficient diffusion in Dell'Omodarme et al. (2012) calculations. The same behaviour appears obviously (the same BCs are used) when considering colour differences at fixed $F606W$ magnitude. Along the unevolved MS, Dell'Omodarme et al. (2012) isochrones are redder by less than 0.01 mag.

Considering a reference magnitude $M_{F606W} = 7$, where the effect of atomic diffusion is negligible, we derive $dY/d(F606W - F814W) = 2.0$ for the Dell'Omodarme et al. (2012) isochrones that translates to an increase of just 10 per cent in the derived ΔY values, compared to our reference calibration.

The VandenBerg et al. (2014) stellar models are calculated with [α/Fe] = 0.4 and the reference solar metal mixture by Asplund et al. (2009). They include the gravitational settling of helium, Li and Be but not of heavy elements. The efficiency of settling from the convective envelope is then moderated as described in VandenBerg et al. (2012). Equation of state and reaction rates for hydrogen burning are also different from our reference calculations (see VandenBerg et al. 2012, for details). The outer boundary conditions for the masses relevant to our analysis are obtained integrating the empirical solar $T(\tau)$ relation by Holweger & Mueller (1974), also different from our reference choice. The adopted BCs are the MARCS BCs by Casagrande & VandenBerg (2014) we have already discussed.

We considered their 12 Gyr, $Z = 0.002$, $Y = 0.25$, 0.29 and 0.33 isochrones to calculate dY/d($F606W - F814W$) and plotted in Fig. 5 the $Y = 0.25$ one. At fixed L, the VandenBerg et al. (2014) is essentially identical to the Dell'Omodarme et al. (2012) counterpart that is slightly cooler than our reference isochrone along the unevolved MS. Moving towards the turn-off, the VandenBerg et al. (2014) isochrone becomes redder than the Dell'Omodarme et al. (2012) counterpart, most probably because of the different implementation of atomic diffusion. The behaviour in the $F606W - (F606W - F814W)$ diagram is, however, different. Because MARCS BCs produce systematically bluer colours (at fixed M_{F606W}) compared to the ATLAS9 BCs (see Fig. 2), the VandenBerg et al. (2014) isochrone appears now bluer than the our reference one (apart from the turn-off region), by about 0.02 mag. Despite this colour difference at fixed Y, we find that the derivative dY/d($F606W - F814W$) (taken at $M_{F606W} = 7$, where the effect of atomic diffusion is negligible) differs by less than 5 per cent, compared to the result with our reference isochrones.

4 SUMMARY

Estimates of the He abundance range ΔY within individual GGCs are crucial to constrain the origin of the multiple population phenomenon and the use of the MS width in optical CMDs is, from the theoretical point of view, a very reliable approach to constrain this quantity. The availability of both UV (from the *HST*-WFC3 camera) and optical (from the *HST*-ACS camera) magnitudes, thanks to the *Hubble Space Telescope* UV Legacy Survey of Galactic GCs project, will allow the homogeneous determination of ΔY for a large sample of GGCs. The UV CMDs can efficiently disentangle the various sub-populations and MS colour differences in the ACS $F606W - (F606W - F814W)$ CMD will allow an estimate of their initial He abundance differences.

We have established here that the dY/d($F606W - F814W$) colour derivative at fixed M_{F606W} (or M_{F814W}) between $\sim$2 and $\sim$3 mag below the MS turn-off is weakly affected by current uncertainties in a range of physics inputs that enter the calculations of stellar models and isochrones, and is completely unaffected by the presence of CNONa abundance anticorrelations.

The value of dY/d($F606W - F814W$) (between) generally decreases with increasing [Fe/H] and, to give a quantitative example, changes by $\sim$25 per cent at $M_{F606W} = 7$ when going from [Fe/H] = -1.6 to -0.7. Table 1 summarizes the results for [Fe/H] ranging between -2.1 and -0.7.

We have found that at our selected [Fe/H] = -1.3 taken as representative of the results that we obtain over all GGC metallicity range, variations by $\pm$0.1 of α_{MLT} around the solar-calibrated value and the use of different $T(\tau)$ relationships to determine the outer boundary conditions for the model calculations leave dY/d($F606W$

Table 1. Derivatives dY/d($F606W - F814W$) for our reference calculations, taken at $\sim$2 and $\sim$3 mag below the $F606W$ turn-off magnitude for an age of 12 Gyr.

Fe/H	dY/d($F606W - F814W$) MS turn-off +1 mag	dY/d($F606W - F814W$) MS turn-off + 2 mag
-2.1	2.3	2.1
-1.6	2.2	1.9
-1.3	2.1	1.8
-1.0	2.0	1.6
-0.7	1.7	1.5

$- F814W$) unchanged, although they change slightly the colours of the isochrones, at the level of at most $\sim$0.02 mag.

Uncertainties due to adopted BCs are not large, in the assumption that our reference ATLAS9, PHOENIX, MARCS and Worthey & Lee (2011) BCs we employed in these comparisons are a fair reflection of current uncertainties. The Worthey & Lee (2011) BCs induce a variation of dY/d($F606W - F814W$) compared to our reference result that causes a decrease of ΔY by 5 per cent if estimated at $M_{F606W} = 6$ and by 16 per cent if estimated at $M_{F606W} = 7$. The PHOENIX and MARCS BCs do not change dY/d($F606W - F814W$).

Just to give an idea of the corresponding variations of the absolute values of ΔY, current estimates provide a typical upper limit $\Delta Y \sim$0.05 (apart from exceptions like NGC 2808 and ω Centauri, see e.g. the data compiled in table 1 of Bastian et al. 2015). A 20 per cent increase or decrease corresponds to variations by at most $\sim$0.01.

If atomic diffusion is fully efficient throughout the star, the value of dY/d($F606W - F814W$) measured at $M_{F606W} = 6$ is affected at the level of at most $\sim$20 per cent, if Y is between 0.35 and 0.40. However, spectroscopic observations of GGC stars have shown that diffusion from the convective envelopes of GGC stars is severely inhibited and when we artificially stop diffusion from the envelope, keeping it efficient only in the underlying radiative layers, we find that dY/d($F606W - F814W$) is unaffected compared to the no-diffusion case.

Finally, the independent isochrone libraries of Dell'Omodarme et al. (2012) and VandenBerg et al. (2014) provide a dY/d($F606W - F814W$) (in the magnitude range where atomic diffusion is negligible) only at most 10 per cent higher than our reference set, despite various differences in the model physics inputs involving the equation of state, outer boundary conditions, nuclear reaction rates and metal abundance mixture.

In summary, we found that the theoretical framework to estimate He variations amongst sub-populations in individual GGCs through MS colour differences is quite robust. Although altering several of the required physics inputs/assumptions can affect the MS colours for a given initial chemical composition, colour differences due to variations of the initial Y abundances are a robust prediction of the current generation of stellar models.

REFERENCES

Angulo C. et al., 1999, Nucl. Phys. A, 656, 3

Asplund M., Grevesse N., Sauval A. J., Scott P., 2009, ARA&A, 47, 481

Bahcall J. N., Pinsonneault M. H., Wasserburg G. J., 1995, Rev. Mod. Phys., 67, 781

Bastian N., Cabrera-Ziri I., Salaris M., 2015, MNRAS, 449, 3333

Bedin L. R., Piotto G., Anderson J., Cassisi S., King I. R., Momany Y., Carraro G., 2004, ApJ, 605, L125

Böhm-Vitense E., 1958, Z. Astrophys., 46, 108

Bragaglia A., Carretta E., Gratton R., D'Orazi V., Cassisi S., Lucatello S., 2010, A&A, 519, A60

Brott I., Hauschildt P. H., 2005, in Turon C., O'Flaherty K. S., Perryman M. A. C., eds, ESA SP-576: The Three-Dimensional Universe with Gaia. ESA, Noordwijk, p. 565

Canuto V. M., Mazzitelli I., 1991, ApJ, 370, 295

Casagrande L., VandenBerg D. A., 2014, MNRAS, 444, 392

Cassisi S., Salaris M., 2013, Old Stellar Populations: How to Study the Fossil Record of Galaxy Formation. Gordon and Breach, New York

Cassisi S., Castellani V., degl'Innocenti S., Weiss A., 1998, A&AS, 129, 267

Cassisi S., Salaris M., Irwin A. W., 2003, ApJ, 588, 862

Cassisi S., Salaris M., Castelli F., Pietrinferni A., 2004, ApJ, 616, 498

Cassisi S., Mucciarelli A., Pietrinferni A., Salaris M., Ferguson J., 2013, A&A, 554, A19

Cox J. P., Giuli R. T., 1968, Principles of Stellar Structure. Wiley-VCH

D'Ercole A., Vesperini E., D'Antona F., McMillan S. L. W., Recchi S., 2008, MNRAS, 391, 825

Dalessandro E., Salaris M., Ferraro F. R., Mucciarelli A., Cassisi S., 2013, MNRAS, 430, 459

Decressin T., Meynet G., Charbonnel C., Prantzos N., Ekström S., 2007, A&A, 464, 1029

Dell'Omodarme M., Valle G., Degl'Innocenti S., Prada Moroni P. G., 2012, A&A, 540, A26

Denissenkov P. A., Hartwick F. D. A., 2014, MNRAS, 437, L21

Denissenkov P. A., VandenBerg D. A., Hartwick F. D. A., Herwig F., Weiss A., Paxton B., 2015, MNRAS, 448, 3314

Dupree A. K., Avrett E. H., 2013, ApJ, 773, L28

Dupree A. K., Strader J., Smith G. H., 2011, ApJ, 728, 155

Girardi L., Castelli F., Bertelli G., Nasi E., 2007, A&A, 468, 657

Gratton R. G. et al., 2001, A&A, 369, 87

Gratton R., Sneden C., Carretta E., 2004, ARA&A, 42, 385

Gratton R. G. et al., 2013, A&A, 549, A41

Grevesse N., Noels A., 1993, in Prantzos N., Vangioni-Flam E., Casse M., eds, Origin and Evolution of the Elements. p. 15

Grevesse N., Asplund M., Sauval A. J., 2007, Space Sci. Rev., 130, 105

Gruyters P., Nordlander T., Korn A. J., 2014, A&A, 567, A72

Holweger H., Mueller E. A., 1974, Sol. Phys., 39, 19

Imbriani G. et al., 2005, Eur. Phys. J. A, 25, 455

King I. R. et al., 2012, AJ, 144, 5

Kippenhahn R., Weigert A., Weiss A., 2012, Stellar Structure and Evolution. Springer-Verlag, Berlin

Krishna Swamy K. S., 1966, ApJ, 145, 174

Lind K., Korn A. J., Barklem P. S., Grundahl F., 2008, A&A, 490, 777

Magic Z., Weiss A., Asplund M., 2015, A&A, 573, A89

Marino A. F., Villanova S., Milone A. P., Piotto G., Lind K., Geisler D., Stetson P. B., 2011, ApJ, 730, L16

Marino A. F. et al., 2012a, A&A, 541, A15

Marino A. F. et al., 2012b, ApJ, 746, 14

Marino A. F. et al., 2014, MNRAS, 437, 1609

Mazzitelli I., D'Antona F., Caloi V., 1995, A&A, 302, 382

Milone A. P. et al., 2012, ApJ, 744, 58

Milone A. P. et al., 2015, ApJ, 808, 51

Moehler S., Dreizler S., Lanz T., Bono G., Sweigart A. V., Calamida A., Nonino M., 2011, A&A, 526, A136

Moehler S., Dreizler S., LeBlanc F., Khalack V., Michaud G., Richer J., Sweigart A. V., Grundahl F., 2014, A&A, 565, A100

Moni Bidin C., Moehler S., Piotto G., Momany Y., Recio-Blanco A., 2007, A&A, 474, 505

Mucciarelli A., Salaris M., Lovisi L., Ferraro F. R., Lanzoni B., Lucatello S., Gratton R. G., 2011, MNRAS, 412, 81

Mucciarelli A., Lovisi L., Lanzoni B., Ferraro F. R., 2014, ApJ, 786, 14

Nardiello D., Milone A. P., Piotto G., Marino A. F., Bellini A., Cassisi S., 2015, A&A, 573, A70

Norris J. E., 2004, ApJ, 612, L25

Pasquini L., Mauas P., Käufl H. U., Cacciari C., 2011, A&A, 531, A35

Pietrinferni A., Cassisi S., Salaris M., Castelli F., 2004, ApJ, 612, 168

Pietrinferni A., Cassisi S., Salaris M., Castelli F., 2006, ApJ, 642, 797

Piotto G. et al., 2007, ApJ, 661, L53

Piotto G. et al., 2015, AJ, 149, 91

Proffitt C. R., Vandenberg D. A., 1991, ApJS, 77, 473

Rogers F. J., Swenson F. J., Iglesias C. A., 1996, ApJ, 456, 902

Salaris M., Cassisi S., 2008, A&A, 487, 1075

Salaris M., Cassisi S., 2015, A&A, 577, A60

Salaris M., Groenewegen M. A. T., Weiss A., 2000, A&A, 355, 299

Salaris M., Weiss A., Ferguson J. W., Fusilier D. J., 2006, ApJ, 645, 1131

Sarajedini A. et al., 2007, AJ, 133, 1658

Sbordone L., Bonifacio P., Castelli F., Kurucz R. L., 2004, Mem. Soc. Astron. Ital. Suppl., 5, 93

Sbordone L., Salaris M., Weiss A., Cassisi S., 2011, A&A, 534, A9

Sirianni M. et al., 2005, PASP, 117, 1049

Tenorio-Tagle G., Munoz-Tunon C., Cassisi S., Silich S., 2016, ApJ, 825, 118

Thoul A. A., Bahcall J. N., Loeb A., 1994, ApJ, 421, 828

VandenBerg D. A., Edvardsson B., Eriksson K., Gustafsson B., 2008, ApJ, 675, 746

VandenBerg D. A., Bergbusch P. A., Dotter A., Ferguson J. W., Michaud G., Richer J., Proffitt C. R., 2012, ApJ, 755, 15

VandenBerg D. A., Bergbusch P. A., Ferguson J. W., Edvardsson B., 2014, ApJ, 794, 72

Villanova S., Geisler D., Piotto G., Gratton R. G., 2012, ApJ, 748, 62

Villante F. L., Serenelli A. M., Delahaye F., Pinsonneault M. H., 2014, ApJ, 787, 13

Worthey G., Lee H.-c., 2011, ApJS, 193, 1

Yong D., Grundahl F., Norris J. E., 2015, MNRAS, 446, 3319

This paper has been typeset from a TeX/LaTeX file prepared by the author.